

# Experimental Implementation of Hogg's Algorithm on a Three-Quantum-bit NMR Quantum Computer

Xinhua Peng<sup>1</sup>, Xiwen Zhu<sup>1\*</sup>, Ximing Fang<sup>1,2</sup>, Mang Feng<sup>1</sup>, Maili Liu<sup>1</sup>, and Kelin Gao<sup>1</sup>

<sup>1</sup>*Laboratory of Magnetic Resonance and Molecular Physics, Wuhan Institute of Physics and Mathematics, The Chinese Academy of Sciences, Wuhan, 430071, People's Republic of China*

<sup>2</sup>*Department of Physics, Hunan Normal University, Changsha, 410081, People's Republic of China*

## Abstract

Using nuclear magnetic resonance (NMR) techniques with three-qubit sample, we have experimentally implemented the highly structured algorithm for the 1-SAT problem proposed by Hogg. A simplified temporal averaging procedure was employed to the three-qubit spin pseudo-pure state. The algorithm was completed with only a single evaluation of structure of the problem and the solutions were found with probability 100%, which outperform both unstructured quantum and the best classical search algorithm.

PACS numbers: 03. 67. Lx, 03.65. -w

Typeset using REVTeX

---

\*Corresponding author. E-mail: xwzhu@nmr.whcnc.ac.cn; Fax: 0086-27-87885291.

## I. INTRODUCTION

Quantum Computers exploiting the principles of quantum parallelism and entanglement of quantum states outperform classical counterparts greatly. Quantum algorithms can solve computational problems much faster than the classical ones [1–4], and can solve even some intractable problems to classical methods, such as the most famous problem of factoring large integers [3]. Hitherto, the selected systems to realize quantum computation have been proposed such as trapped ions [5,6], quantum dots [7], and cavity quantum-electrodynamics [8,9]. However, the most effective one to realize quantum algorithms to date is the liquid-state NMR spins [10,11]. Several quantum algorithms have been implemented by liquid-state NMR ensemble including the Deutsch-Jozsa algorithm with two, three [14–18] and five [19] qubits, the Grover’s algorithm with two [20,21] and three qubits [22], an algorithmic benchmark [23], an order-finding algorithm with five qubits [24].

Search algorithm is one of the most important algorithms. The difference between quantum and classical search algorithms is that, quantum ones can operate simultaneously on a superposition of all possible search states so as to be superior to classical counterparts greatly. A quantum search algorithm that uses the underlying structure of the search problem to establish correlations between problem properties and the solutions results in a substantial improvement over a search one that ignores them, such as Hogg’s algorithm [25] vs. Grover’s one [4]. However, when only two qubits are considered, there is no difference between Hogg’s algorithm and Grover’s one because both of the algorithms only require one search step. For  $n > 2$  qubits, the superiority of Hogg’s algorithm will be displayed, which still require a single step, while Grover’s one requires  $\sqrt{2^n}$  steps. For example, when  $n = 3$  qubits, Grover’s algorithm needs at least 2 steps with probability near 95%. Hogg’s algorithm for 2-qubit has been implemented in Ref. [26]. In this paper, we experimentally implemented the Hogg’s algorithm for a 1-SAT with the 3-qubit pseudo-pure state prepared by three-step temporal averaging.

## II. THE HIGHLY STRUCTURED ALGORITHM

The highly structured algorithm is associated with the satisfiability problem (SAT) [27], one of the most difficult class of non-deterministic polynomial problem (NP) [27]. A SAT is a combinatorial search problem [27], consisting of a logic formula in  $n$  boolean variables (true or false)  $V_1, \dots, V_n$  and the requirement to find an assignment, specifying a value for each boolean variable, that makes the formula true. The logic formula can be expressed as a conjunction of  $m$  clauses and each clause is a disjunction of some variables, any of which may be negated. When all the clauses have  $k$  variables, the problem is called  $k$ -SAT. In general, the computational cost of solving a SAT grows exponentially with  $n$  in the worst case. For  $k \geq 3$ ,  $k$ -SAT is NP-complete. However, for 1-SAT and maximally constrained  $k$ -SAT, Hogg proposed a quantum algorithm to find a solution in one step by using problem structure. As each false clause for a given assignment is counted as a conflict, solutions are assignments with no conflict. Therefore, the correlations between problem properties and the assignments are set up so that Hogg's algorithm can solve problems with only a single testing of all the assignments, corresponding to a single classical search step.

For a 1-SAT problem with  $n$  variables and  $m$  clauses, in fact, the algorithm takes the following four stages [25].

1. Initialize the amplitude equally among the states, giving an equal superposition of bases  $|s\rangle$ ,  $|\psi_i\rangle = 2^{-\frac{n}{2}} \sum_s |s\rangle$ , with bit strings  $s$  being all  $2^n$  assignments of  $n$  variables.

2. Adjust the phases of  $|s\rangle$  based on the conflicts  $c$  in the assignments  $s$ , ranging from 0 to  $m$ , i.e., apply a transformation  $R$  on  $|\psi_i\rangle$ , where  $R$  is a diagonal matrix with elements

$$R_{ss} = \begin{cases} \sqrt{2} \cos[(2c - 1)\frac{\pi}{4}], & \text{for even } m; \\ i^c, & \text{for odd } m. \end{cases} \quad (1)$$

3. Mix the amplitudes from different assignments with the mixing matrix  $U$  depending only on the Hamming distance  $d$  between  $r$  and  $s$  is described as

$$U_{rs} = U_{d(r,s)} = \begin{cases} 2^{-\frac{n-1}{2}} \cos[(n - m + 1 - 2d)\frac{\pi}{4}], & \text{for even } m; \\ 2^{-\frac{n}{2}} e^{i\pi(n-m)/4} (-i)^d, & \text{for odd } m. \end{cases} \quad (2)$$

Here,  $d(r, s) = |r| + |s| - 2|r \wedge s|$  with  $|r|$  ( $|s|$ ) being the number of 1-bits in  $r$  ( $s$ ) and  $|r \wedge s|$ , the number of 1-bits both assignments have in common. The operator  $U$  can be defined in terms of two simpler operations:  $U = W\Gamma W$ , where  $W = 2^{-\frac{n}{2}}(-1)^{|r \wedge s|}$  is the Walsh-Hadamard transform,  $\Gamma$ , and  $\Gamma$  is a diagonal matrix with elements

$$\Gamma_{rr} = \gamma(r) = \gamma_h = \begin{cases} \sqrt{2} \cos[(m - 2h - 1)\frac{\pi}{4}], & \text{for even } m; \\ i^h e^{-i\pi m/4}, & \text{for odd } m. \end{cases} \quad (3)$$

depending only on the number of 1-bits in each assignments  $h = |r|$ , ranging from 0 to  $m$ .

4. Measure the final superposition  $|\psi_f\rangle = UR|\psi_i\rangle$ .

For our 3-spin system (i. e.  $n = 3$ ), the number of clauses,  $m$ , in the 1-SAT formula can be 3, 2, or 1. The quantum circuit for the highly structure search in a 3-qubit system is shown in Fig. 1. According to four stages of the Hogg's algorithm above, the calculation starts with a Walsh-Hadamard transform  $W$  applying to a pseudo-pure state  $|000\rangle$ , to prepare the equal superposition state  $|\psi_i\rangle$ , where  $W = H_A \otimes H_B \otimes H_C$ , with  $H = X^2Y$  (pulses applied from right to left) being a single-spin Hadamard gate. Then we derived the NMR pulse sequences for  $R$  and  $U$  in Eqs. (1) and (2). We take the 1-SAT with  $m = 3$ , i.e., the logic formula being  $V_1 \wedge V_2 \wedge V_3$ , as an example. In this case,  $U$  could be represented by  $W\Gamma W$ . From Eqs. (1) and (3), the expressions for  $R$  and  $\Gamma$  can be written into

$$\text{diag}[R_{V_1 \wedge V_2 \wedge V_3}] = [-i, -1, -1, i, -1, i, i, 1], \quad (4)$$

$$\text{diag}[\Gamma_{m=3}] = [1, i, i, -1, i, -1, -1, -i]. \quad (5)$$

which correspond to the pulse sequences  $R_{V_1 \wedge V_2 \wedge V_3} \sim \bar{Z}_1 \bar{Z}_2 \bar{Z}_3$ ,  $\Gamma_{m=3} \sim Z_1 Z_2 Z_3$  (up to an irrelevant overall phase factor). In order to make the best use of the available coherence time and to diminish errors due to the increased number of RF pulses, the pulse sequences of  $W$ ,  $R$  and  $\Gamma$  were optimized to eliminate unnecessary operations with the help of NMR principle [28]. Two instances for  $m = 1$  and 3 were chosen for demonstrating Hogg's algorithm in our experiments for their simple pulse

sequences. All the reduced pulse sequences for all possible formulas with  $m = 1$  and 3 as well as theoretical solutions are listed in Table. 1.

### III. THE NMR EXPERIMENTAL RESULTS

The Hogg's algorithm was implemented by liquid-state high-resolution NMR spectroscopy with carbon-13 labeled alanine  $NH_3^+ - C^\alpha H(C^\beta H_2) - C' O_2^-$  dissolved in  $D_2O$ . We chose  $C'$ ,  $C^\alpha$  and  $C^\beta$  as the three-spin system in experiments, representing spin 1, spin 2 and spin 3, respectively. Spectra were recorded on a Bruker ARX500 spectrometer with a probe tuned at 125.77MHz for  $^{13}C$ . The chemical shifts of three different carbon spins were calibrated about  $-4320$ ,  $0$ , and  $15793$ Hz, and the spin-spin coupling constants  $J_{12}$ ,  $J_{23}$ , and  $J_{13}$ ,  $34.94$ ,  $53.81$ , and  $1.21$ Hz, respectively. The relaxation times were measured to be  $T_1(1) = 20.3$  sec,  $T_1(2) = 2.8$  sec, and  $T_1(3) = 1.5$  sec and  $T_2(1) = 1.3$  sec,  $T_2(2) = 0.41$  sec, and  $T_2(3) = 0.81$  sec [18]. Protons were decoupled during the whole experiments, using a standard heteronuclear decoupling technique. Spin-selective excitations were executed using low-power, long-duration pulses with a *Gaussian* shape. The length of these pulses was tailored to achieve sufficient selectivity in the frequency domain without disturbing the nearest nucleus, depending on the difference of the chemical shifts between nuclei. We took the length of the selective pulses to be  $0.7$ ms and the excitation power to be  $29.6$ dB for selective  $\frac{\pi}{2}$  pulses for all  $^{13}C$  nuclei.

#### A. The preparation of pseudo-pure states

In liquid-state NMR ensemble quantum computers, Chuang et al. [11] proposed pseudo-pure states instead of the genuine pure states as the initial state. Several methods have been proposed to prepare the pseudo-pure states including spatial averaging [10], temporal averaging [13], logical labeling [11,30,29]. Recently, an alternative simplified temporal averaging was proposed by Lieven et al. [24]. For a  $n$ -qubits homonuclear system, the deviation density matrix of the system in thermal equilibrium is a sum of  $n$  terms,

$$\rho_{eq} = \sum_{k=1}^n I_{kz}. \quad (6)$$

The deviation density matrix of the desired pseudo-pure state  $|00\dots 0\rangle$  is

$$\rho_{eff} = \sum_{k=1}^n I_{kz} + \sum_{l>k=1}^n I_{kz}I_{lz} + \sum_{m>l>k=1}^n I_{kz}I_{lz}I_{mz} + \dots, \quad (7)$$

a sum of  $2^n - 1$  terms. In order to obtain the desired pseudo-pure state,  $[(2^n - 1)/n]$  different experiments are at least needed by utilizing controlled-NOT ( $CN_{ij}$  flips spin  $j$  if and only if  $i$  is  $|1\rangle$ ) and NOT ( $N_i$  flips the sign of spin  $i$ ).

For a homonuclear 3-spin system, (i.e.  $n = 3$ ), three separate experiments are at least required to achieve the pseudo-pure state  $\rho_{000}$ . We use 3 separate experiments, giving a total of 9 product operator terms. The 2 extra of 9 terms are canceled out pairwise by using NOT ( $N_i$ ) operations. The procedure can be chosen in a variety of ways. For different samples, one can choose an optimal experimental scheme. As to our sample of alanine with  $1/2J_{13} = 0.41$  sec, which is comparable to the smallest  $T_2$ , gate  $CN_{13}$  or  $CN_{31}$  containing the evolution under the scalar coupling  $J_{13}$  should be excluded in the preparation circuit. We choose the following 3 states preparation sequences acting on the equilibrium as

$$E, \quad CN_{32}CN_{21}N_3, \quad CN_{21}CN_{12}CN_{32} \quad (8)$$

where  $E$  is unit matrix denoting no operation. The corresponding product operators of the 3 states are

$$\begin{aligned} \rho_1 &= I_{1z} + I_{2z} + I_{3z} \\ \rho_2 &= 4I_{1z}I_{2z}I_{3z} + 2I_{2z}I_{3z} - I_{3z} \\ \rho_3 &= 2I_{1z}I_{3z} + 2I_{1z}I_{2z} + I_{3z} \end{aligned} \quad (9)$$

The sum of the 3 states is

$$\rho_{sum} = \rho_1 + \rho_2 + \rho_3 = I_{1z} + I_{2z} + I_{3z} + 2I_{1z}I_{3z} + 2I_{1z}I_{2z} + 2I_{2z}I_{3z} + 4I_{1z}I_{2z}I_{3z} \quad (10)$$

It can be seen from Eq. (7) and Eq. (10) that  $\rho_{sum}$  is the same as  $\rho_{eff}$  for  $n = 3$ . The experimental pulse sequences was shown in Fig. 1. Of course, the same result to exclude this  $1/2J_{13}$  evolution can also be gained by swapping gates proposed by Collins et al. [18], but it is more complex to implement experimentally. Note that a magnetic field gradient

pulses were accomplished at the end of the experiments in order to eliminate the residual transverse magnetic vectors and thereby reduce the errors.

The pseudo-pure state  $\rho_{000}$  was achieved in the experiment, by summing the three experimental results, where the qubits from high to low corresponds to spin 1, 2 and 3, respectively. The resultant spectra of the three spectra then recorded (shown in Fig.2) through reading-out pulses confirm that a pseudo-pure state  $\rho_{000}$  has been prepared. The normalized diagonal elements of the deviation matrix  $\rho_{000}$  for the pseudo-pure state  $|000\rangle$  by quantum state tomography [30] was given as

$$diag[\rho_{000}] = [1.000, 0.0314, -0.0291, -0.0032, 0.0520, 0.0114, -0.0535, -0.0277] \quad (11)$$

All diagonal elements except one with the value of 1 in Eq. (11) should be zero theoretically. So the maximal relative error of the experimental values of the diagonal elements was shown to be  $< 6\%$ , with the small off-diagonal elements.

Similarly, the procedure can be applied to a homonuclear 4-spin system (i. e.  $n = 4$ .) To obtain the pseudo-pure state  $\rho_{0000}$ , we can perform 5 experiments as follows

$$\begin{aligned} & CN_{12}CN_{14}CN_{31}, \quad CN_{21}CN_{42}CN_{34}, \quad CN_{12}CN_{42} \\ & CN_{12}CN_{14}N_3, \quad CN_{23}CN_{24}N_{31} \end{aligned} \quad (12)$$

Among a total of 20 terms produced, the 4 extra terms can be eliminated pairwise through  $N_i$  operations and one extra term removed through the magnetic field gradient technique. For a homonuclear 5-spin system, the procedure has clearly been demonstrated in Ref. [24].

### B. The NMR results of the highly structure algorithm

Applying the pulse sequences in Table. I. to the pseudo-pure state  $\rho_{000}$ , we got the results of Hogg's algorithm. For  $m = 3$ , because only the diagonal elements are non-zeros, we reconstructed the normalized diagonal elements like the  $\rho_{000}$  preparation above. The experimental deviation matrixes were obtained respectively

$$\begin{aligned}
diag[\rho_{V_1 \wedge V_2 \wedge V_3}] &= [-0.0190, 0.0297, -0.0582, 0.0631, -0.0072, 0.0416, -0.0800, 1.0000], \\
diag[\rho_{\bar{V}_1 \wedge V_2 \wedge V_3}] &= [0.0087, -0.0074, 0.0959, -0.0845, 0.0105, -0.0056, 1.0000, -0.0393], \\
diag[\rho_{V_1 \wedge \bar{V}_2 \wedge V_3}] &= [-0.0412, 0.0716, -0.0149, 0.0187, -0.0580, 1.0000, -0.0047, 0.0289], \\
diag[\rho_{V_1 \wedge V_2 \wedge \bar{V}_3}] &= [0.0037, 0.0340, -0.0186, 1.0000, -0.0211, 0.0092, -0.0670, 0.0881], \\
diag[\rho_{\bar{V}_1 \wedge \bar{V}_2 \wedge V_3}] &= [0.0512, 0.0077, -0.157, -0.0269, 1.0000, -0.0127, 0.0029, -0.0082], \\
diag[\rho_{\bar{V}_1 \wedge V_2 \wedge \bar{V}_3}] &= [0.0173, 0.0171, 1.0000, -0.0348, -0.0091, -0.0092, 0.0606, -0.0093], \\
diag[\rho_{V_1 \wedge \bar{V}_2 \wedge \bar{V}_3}] &= [-0.0304, 1.0000, -0.0197, 0.0200, -0.0228, 0.0594, -0.0199, 0.0199], \\
diag[\rho_{\bar{V}_1 \wedge \bar{V}_2 \wedge \bar{V}_3}] &= [1.0000, 0.0314, -0.0291, -0.0032, 0.0520, 0.0114, -0.0535, -0.0277].
\end{aligned} \tag{13}$$

In contrast with the theoretical expectation, the maximal relative errors of the experimental values of the diagonal elements was shown to be  $< 9\%$ , with the small off-diagonal elements.

For  $m = 1$ , we reconstructed the experimental final deviation matrices by quantum state tomography. In Fig. 4 were shown the theoretical and measured results for these cases with the maximal relative errors  $16\% \sim 25\%$  of the density matrix elements. It can be seen clearly from Eq. (13) and Fig. 4 that the experimental results are in good agreement with the theory. Errors are primarily due to inhomogeneity of RF fields and static magnetic fields, magnetization decay during the measurement and imperfect calibration of the rotations.

#### IV. DISCUSSION

In summary, we have experimentally demonstrated a NMR realization of quantum algorithm for a highly structured searching problem on a three-qubit quantum computer. The simplified temporal averaging for preparing the pseudo-pure states takes less separate experiments than the original temporal averaging proposed by Knill et al. [13], e. g., 3 times instead of 7 times for a 3-spin system. Moreover, its Signal-to-Noise ratio is better than that of spatial averaging [10,12]. Hogg's algorithm for 3 qubits was completed on the prepared pseudo-pure state  $\rho_{000}$ , unlike some algorithms only on the thermal state, and the final results were also read out by a weak measurement on the ensemble, which accomplish



the whole process of quantum computation.

Hogg's algorithm based on the structure of a problem, with a particular choice of the phases determined by the number of conflicts in assignments, finds the solutions to 1-SAT problem in a single step with probability 100% even for  $n \rightarrow \infty$ . By contrast, the unstructured search methods require  $O(2^n)$  steps classically, and  $O(2^{n/2})$  steps on quantum computers [4]. For example, in the 3-qubit Grover's algorithm NMR experiment implemented by Vandersypen et al. [22] with a heteronuclear system, per Grover iteration applied 19 pulses, 2 evolutions of  $1/2J$  and 3 of  $1/4J$  and performed 2 iterations at least to find a single solution  $|x_0\rangle$ . Comparing our pulse sequences with it, Hogg's algorithm adopts far less RF pulses and requires far less coherence time so as to be realized more easily. In addition, probability 100% guarantees that Hogg's algorithm is a complete method, i. e. failure to find a solution definitely indicates the problem is not soluble. Unlike the previously proposed quantum algorithms, such as the Grover's algorithm [4], that find solutions with probability less than one, cannot guarantee no solutions existing. Hogg's algorithm is more efficient to solve any 1-SAT problem. Furthermore, this algorithm also applied to maximally constrained soluble  $k$ -SAT problems [25] for any  $k$  with an analogue procedure. To experimentally implement this algorithm for larger systems, the main difficulties are to address and control the qubits well and to maintain coherence during the computational process.

## ACKNOWLEDGEMENTS

We thank Xiaodong Yang, Hanzheng Yuan, Xu Zhang and Guang Lu for help in the course of experiments.

## REFERENCES

- [1] D. Deutsch, and R. Jozsa, Proc. Roy. Soc. Lond. A, 439, 553 (1992).
- [2] R. Cleve, A. Ekert, C. Macchiavello and M. Mosca, Proc. Roy. Soc. Lond. A, 454, 339 (1998).
- [3] P. Shor, Algorithms for quantum computation: discrete logarithms and factoring. proc. 35th Annu. Symp. on Found. of Computer Science, (IEEE comp. Soc. Press, Los Alamos, CA. 1994) 124-134.
- [4] L. K. Grover, Phys. Rev. Lett. 79, 325 (1997).
- [5] J. Cirac and P. Zoller, Phys. Rev. Lett. 74, 4091 (1995).
- [6] C. Monroe, D. M. Meekhof, B. E. King, W. M. Itano, and D. J. Wineland, Phys. Rev. Lett. 75, 4714 (1995).
- [7] S. Bandyopadhyay and V. Roychowdhury, Jpn. J. Appl. Phys. 35, 3550 (1996).
- [8] P. Domokoss, J. M. Raimond, M. Brune, S. Haroche, Phys. Rev. Lett. 52, 3554 (1995).
- [9] Q. A. Turchette, C. J. Hood, W. Lange, H. Mabuchi, and H. J. Kimble, Phys. Rev. Lett, 75, 4710 (1995).
- [10] D. G. Cory, A. F. Fahmy and T. F. Havel, Proc. Natl. Acad. Sci. USA 94 (1997) 1634 .
- [11] N. Gershenfeld and I. L. Chuang, Science 275, 350 (1997).
- [12] D.G. Cory, M. D. Price and T. F. Havel, Physica D 120 (1998) 82.
- [13] E. Knill, I. Chuang and R. Laflamme, Phys. Rev. A 57 (1998) 3348.
- [14] I. L. Chuang, L. M. K. Vandersypen, X. Zhou, D. W. Leung, S. Lloyd, Nature 393, 143 (1998).
- [15] J. A. Jones and Mosca, J. Chem. phys. 109, 1648 (1998).

- [16] N. Linden, H. Barjat and R. Freeman, *Chem. Phys. Lett.* 80, 3408, 229 (1998).
- [17] J. Kim, J.-S. Lee and S. Lee, *Phys. Rev. A* 62, 022312 (2000).
- [18] D. Collins, K. W. Kim, W. C. Holton, H. sierzputowska-Gracz, and E. O. Stejskal, *Phys. Rev. A* 62, (2000).
- [19] R. Marx, A. F. Fahmy, J. M. Myers, W. Bermel and s. J. Glaser, *Phys. Rev. A* 62, 012310 (2000).
- [20] I. L. Chuang, N. Gershenfeld and M. Kubinec, *Phys. Rev. Lett.* 80, 3408 (1998).
- [21] J. A. Jones, m. Mosca and R. H. Hansen, *Nature* 393. 344 (1998).
- [22] L. M. K. Vandersypen et al., *Appl. Phys. Lett.* 76, 646 (2000).
- [23] E. Knill, R. Laflamme, R. Martinez and C.-H. tsieng, *Nature* 404, 368 (2000).
- [24] Lieven M. K, Vandersypen, Matthias Steffen, and Gregory Breyta, *Phys. Rev. Lett.* 85, 5452 (2000).
- [25] T.Hogg, *Phys. Rev. Lett.* 80 (1998) 2473.
- [26] X. Zhu, X. Fang, M. Feng, F. Du, K. Gao, and X. Mao, *Physica D* 156, 179 (2001).
- [27] M. R. Garey and D. S. Johnson, *Computers and Intractability: a Guide to the Theory of NP-Completeness*, Freeman, San Francisco, (1979).
- [28] R. Ernst, G. Bodenhausen and A. Wokaun, *Principles of Nuclear Magnetic Resonance in One and Two Dimensions* (Oxford Univ. Press, Oxford, 1990).
- [29] K. Dorai, Arvind and A. Kumar, *Phys. Rev. A* 61 (2000) 042306.
- [30] I. L. Chuang, N. Gershenfeld, M. Kubinec and D. Leung, *Proc. Roy. Soc.Lond A* 454 (1998) 447.
- [31] I. L. Chuang, and Y. Yamamoto, *Phys. Rev. A* 52, 3489 (1995).

[32] J. A. Jones, *Science* 280, 229 (1998).

## Captions of the figures

Fig. 1 Quantum circuit for 3-qubits that implements a highly structure search algorithm. Horizontal lines represent qubits, time goes from left to right. Using three Hadamard gates, an pseudo-pure states  $|\psi_0\rangle = |000\rangle$  is transformed into a uniform superposition state  $|\psi_i\rangle$ , which is then converted to the answer state  $|\psi_f\rangle$  after the action of gates  $R$  and  $U$ . For the definition of  $R$  and  $U$ , see text.

Fig. 2 NMR pulse sequences to implement the pseudo-pure state  $\rho_{000}$ . Narrow and wide boxes correspond to  $\frac{\pi}{2}$  and  $\pi$  pulses (refocusing pulses) respectively.  $X$  and  $Y$  denote the pulses along the x- and y-axis,  $\bar{X}$  and  $\bar{Y}$ , opposite to the x- and y-axis. (a) to prepare the state of  $\rho_2$  in Eq. (4). (b) to prepare the state of  $\rho_3$  in Eq. (4).  $\rho_1$  is the thermal equilibrated state, no operation). The pulse sequences are designed for alanine with small  $J_{13}$ .

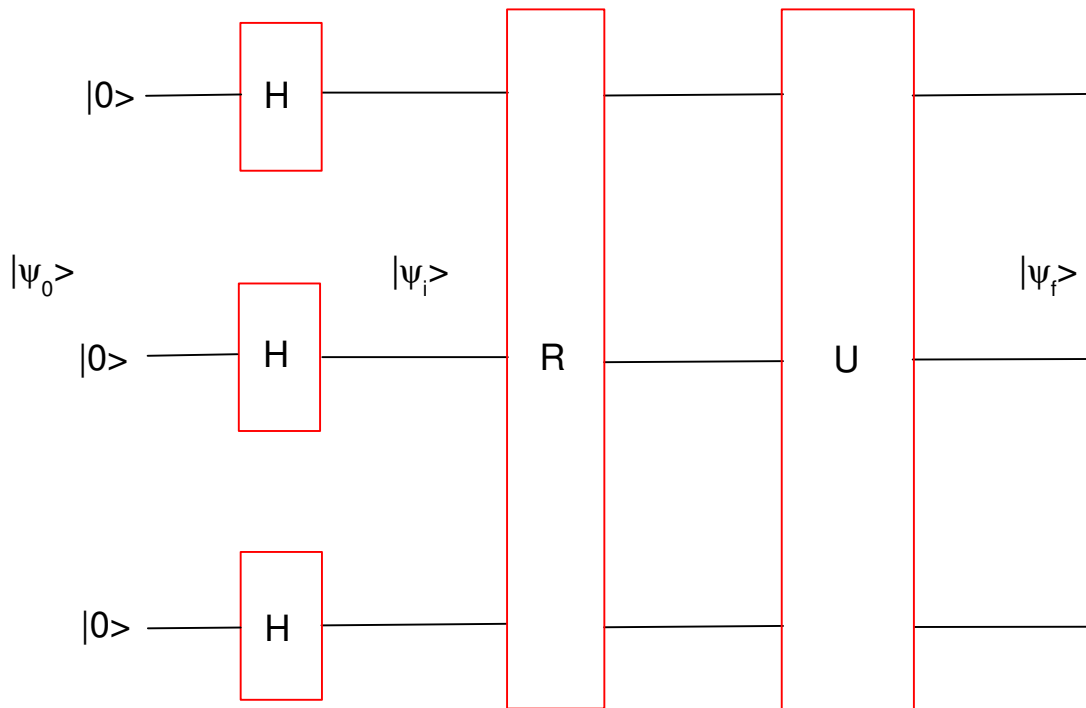
Fig. 3 The resultant  $^{13}\text{C}$  spectra of three experimentally measure spectra of the prepared pseudo-pure state  $\rho_{000}$ . The reading-out pulses (a)  $[\frac{\pi}{2}]_y^1$ , (b)  $[\frac{\pi}{2}]_y^2$ , (c)  $[\frac{\pi}{2}]_y^3$  were applied respectively. The abscissa indicates the frequency, and the ordinate denotes the intensity of the spectra (in arbitrary unit).

Fig. 4 Experimental and theoretical deviation density matrices (in arbitrary units) for the Hogg's algorithm of all logic formulas when  $m = 1$ . (a)—(f) represent the recovered matrices for the logic formula  $V_1, \bar{V}_1, V_2, \bar{V}_2, V_3, \bar{V}_3$ , respectively, the left and right column denoting the real and imaginary components. (a1)—(f1) are the corresponding theoretical values. Relative errors are shown as percentages.

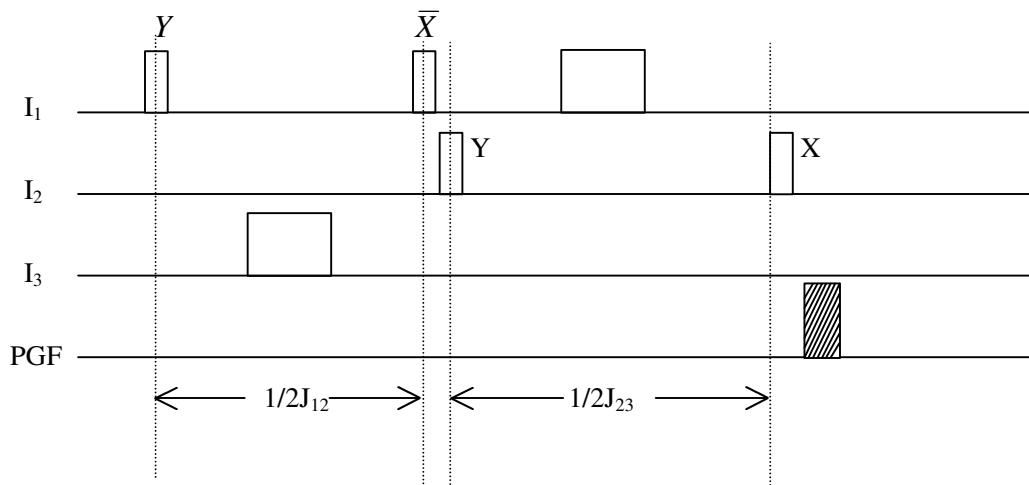
### Captions of the tables

Table. I All the logic formulas for 1-SAT of a 3-spin system for  $m = 1$  or  $3$ , the corresponding theoretical solutions and the reduced pulse sequences for the operator  $URW$ , where the logic variables with subscript  $i$  stand for spin  $i$ .  $X$  and  $Y$  denote the  $\frac{\pi}{2}$  pulses along the x- and y-axis,  $\bar{X}$  and  $\bar{Y}$ , opposite to the x- and y-axis. The subscripts represent the qubits.

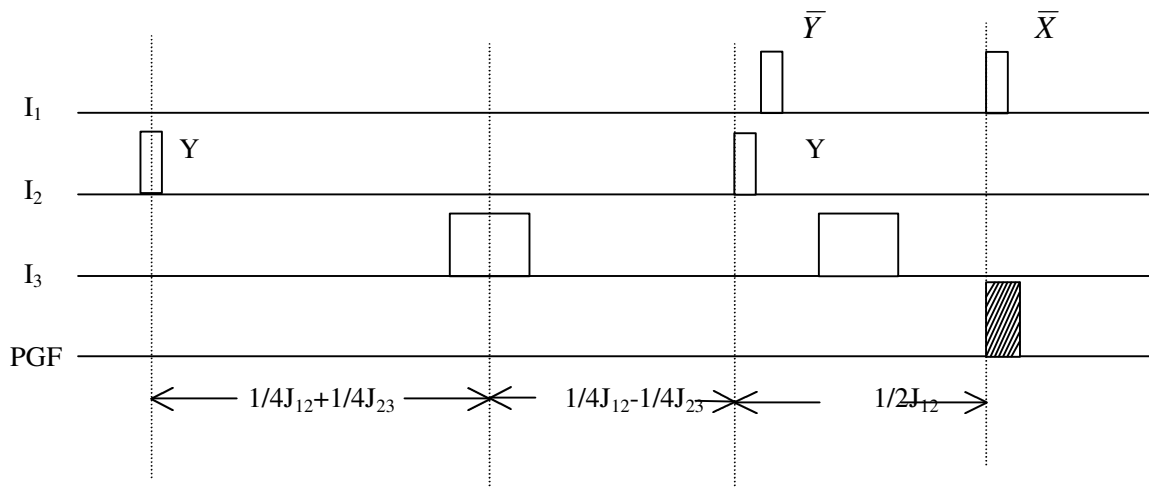
$m$	the logic formula	the corresponding theoretical solutions	the corresponding reduced pulses sequence for $URW$
1	$V_1$	$ 001\rangle +  011\rangle +  101\rangle +  111\rangle$	$X_1^2 Y_2 Y_3$
	$\bar{V}_1$	$ 000\rangle +  010\rangle +  100\rangle +  110\rangle$	$Y_2 Y_3$
	$V_2$	$ 010\rangle +  011\rangle +  110\rangle +  111\rangle$	$Y_1 X_2^2 Y_3$
	$\bar{V}_2$	$ 000\rangle +  001\rangle +  100\rangle +  101\rangle$	$Y_1 Y_3$
	$V_3$	$ 100\rangle +  101\rangle +  110\rangle +  111\rangle$	$Y_1 Y_2 X_3^2$
	$\bar{V}_3$	$ 000\rangle +  001\rangle +  010\rangle +  011\rangle$	$Y_1 Y_2$
3	$V_1 \wedge V_2 \wedge V_3$	$ 111\rangle$	$(X\bar{Y}X)_1(X\bar{Y}X)_2(X\bar{Y}X)_3$
	$\bar{V}_1 \wedge V_2 \wedge V_3$	$ 110\rangle$	$(X\bar{Y}\bar{X})_1(X\bar{Y}X)_2(X\bar{Y}X)_3$
	$V_1 \wedge \bar{V}_2 \wedge V_3$	$ 101\rangle$	$(X\bar{Y}X)_1(X\bar{Y}\bar{X})_2(X\bar{Y}X)_3$
	$\bar{V}_1 \wedge \bar{V}_2 \wedge V_3$	$ 100\rangle$	$(X\bar{Y}\bar{X})_1(X\bar{Y}\bar{X})_2(X\bar{Y}X)_3$
	$V_1 \wedge V_2 \wedge \bar{V}_3$	$ 011\rangle$	$(X\bar{Y}X)_1(X\bar{Y}X)_2(X\bar{Y}\bar{X})_3$
	$\bar{V}_1 \wedge V_2 \wedge \bar{V}_3$	$ 010\rangle$	$(X\bar{Y}\bar{X})_1(X\bar{Y}X)_2(X\bar{Y}\bar{X})_3$
	$V_1 \wedge \bar{V}_2 \wedge \bar{V}_3$	$ 001\rangle$	$(X\bar{Y}X)_1(X\bar{Y}\bar{X})_2(X\bar{Y}\bar{X})_3$
	$\bar{V}_1 \wedge \bar{V}_2 \wedge \bar{V}_3$	$ 000\rangle$	$(X\bar{Y}\bar{X})_1(X\bar{Y}\bar{X})_2(X\bar{Y}\bar{X})_3$



**Fig. 1** xhpeng et al.



(a)



(b)

**Fig .2 xhpeng et al.**



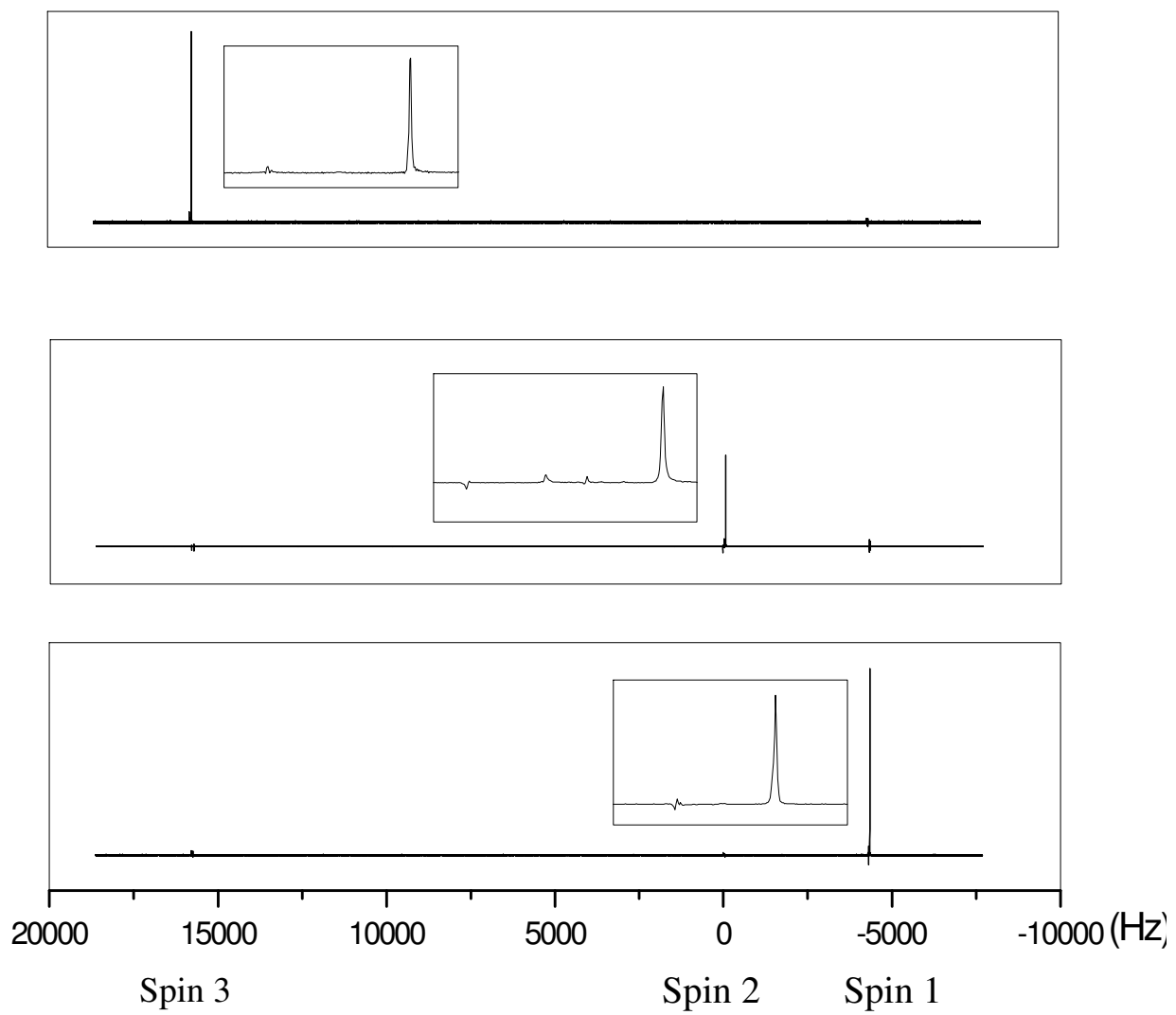


**Fig. 3 xhpeng et al.**

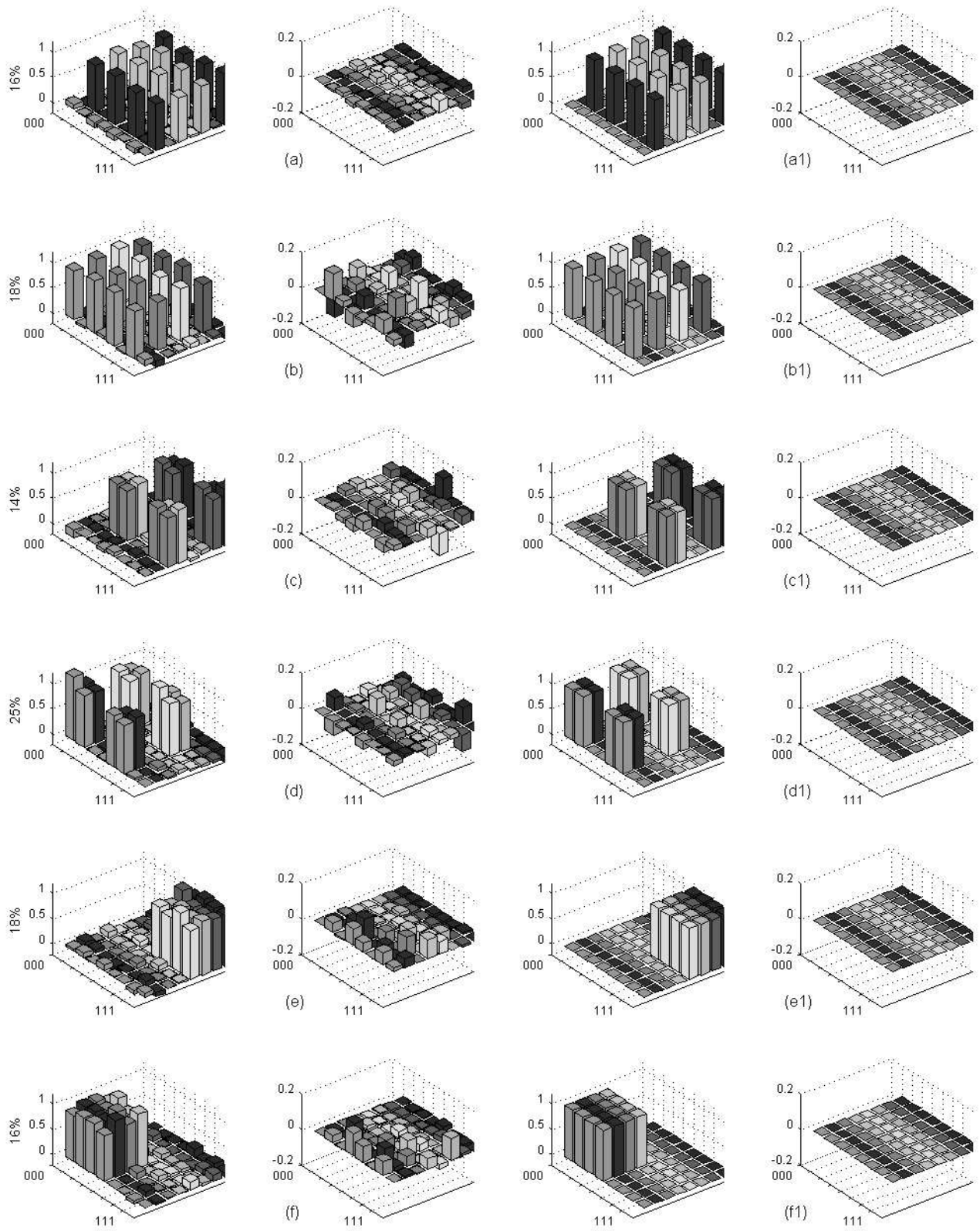


Fig. 4. xhpeng et al.

